

# Parallel MR Imaging: A User's Guide<sup>1</sup>

*James F. Glockner, MD, PhD • Houchun H. Hu, BME • David W. Stanley, BS • Lisa Angelos, PhD • Kevin King, PhD*

Parallel imaging is a recently developed family of techniques that take advantage of the spatial information inherent in phased-array radiofrequency coils to reduce acquisition times in magnetic resonance imaging. In parallel imaging, the number of sampled k-space lines is reduced, often by a factor of two or greater, thereby significantly shortening the acquisition time. Parallel imaging techniques have only recently become commercially available, and the wide range of clinical applications is just beginning to be explored. The potential clinical applications primarily involve reduction in acquisition time, improved spatial resolution, or a combination of the two. Improvements in image quality can be achieved by reducing the echo train lengths of fast spin-echo and single-shot fast spin-echo sequences. Parallel imaging is particularly attractive for cardiac and vascular applications and will likely prove valuable as 3-T body and cardiovascular imaging becomes part of standard clinical practice. Limitations of parallel imaging include reduced signal-to-noise ratio and reconstruction artifacts. It is important to consider these limitations when deciding when to use these techniques.

©RSNA, 2005

**Abbreviations:** FOV = field of view, GRAPPA = generalized autocalibrating partially parallel acquisition, SE = spin echo, SENSE = sensitivity encoding, SNR = signal-to-noise ratio, SPGR = spoiled gradient echo, 3D = three-dimensional, TR = repetition time, 2D = two-dimensional

**RadioGraphics 2005; 25:1279-1297 • Published online 10.1148/rg.255045202 • Content Codes:** **MR** **PH**

<sup>1</sup>From the Department of Radiology, Mayo Clinic, 200 First St SW, Rochester, MN 55905 (J.F.G., H.H.H.); and GE Medical Systems, Milwaukee, Wis (D.W.S., L.A., K.K.). Recipient of a Certificate of Merit award for an education exhibit at the 2003 RSNA Annual Meeting. Received November 10, 2004; revision requested January 4, 2005; revision received and accepted March 30. J.F.G. and H.H.H. have no financial relationships to disclose. Address correspondence to J.F.G. (e-mail: [glockner.james@mayo.edu](mailto:glockner.james@mayo.edu)).

©RSNA, 2005

## Introduction

The recent history of magnetic resonance (MR) imaging has in large part been devoted to finding ways to increase acquisition speed. Although impressive gains have been made and the acquisition times of many sequences have been reduced from minutes to seconds, some fundamental limitations have been reached due to technical and physiologic problems associated with rapidly switching gradients. Recently, parallel imaging has emerged as a technique that can surmount many of these obstacles. Instead of relying on faster and stronger gradients for improvements in acquisition time, the inherent spatial sensitivity of the phased-array coils is used to provide some of the spatial information in the image that would otherwise be obtained in the traditional manner of Fourier transform MR imaging. In other words, parallel imaging allows a reduction in the number of phase-encoding steps while still producing images of reasonable quality and spatial resolution. Parallel imaging increases the acquisition speed by factors of 1.5 to 3 in most commercially available applications. In theory, much higher gains are possible, but they are currently limited by artifact and signal-to-noise ratio (SNR) considerations.

The most obvious clinical application of parallel imaging is simply to shorten the acquisition time of a sequence. This is particularly important for body and cardiovascular imaging, where breath holding is both frequently required and a frequent source of patient complaint. Certainly, the distinction between an acquisition beyond a patient's endurance and one comfortably within his or her breath-hold capacity is a critical one in terms of image quality. However, these gains in acquisition speed can also be used for other purposes; for example, instead of decreasing the acquisition time, the increased speed can be used to improve spatial resolution in the same amount of time. Likewise, fast spin-echo (SE) and single-shot fast SE sequences can be improved by reducing echo train lengths and thereby diminishing image blurring. Parallel imaging is highly flexible and can be combined with virtually any pulse sequence. The combination of parallel imaging with other fast imaging methods is also possible, and these techniques will be useful for applications in real-time and interventional MR imaging.

This article provides a brief explanation of the fundamental concepts of parallel imaging and then illustrates some of the potential clinical applications of this technique. Body and cardiovascular applications are emphasized.

## Background and History

Phased-array coils were initially developed to improve SNR in MR imaging by reducing coil size and sensitive volume, which effectively reduces the amplitude of the noise detected. Multiple overlapping small coils can cover the same volume as a larger coil, and when the signals from individual coils are combined, the noise is substantially reduced and SNR is significantly improved.

Soon after the introduction of phased-array coils, however, it was recognized that they could also be used to reduce acquisition time by sampling the MR signal in a parallel fashion (1–5). The basis of these techniques is the concept that acquisition time is proportional to the number of phase-encoding lines in a Cartesian acquisition. Increasing the distance between phase-encoding lines in k-space by a factor  $R$  while keeping the spatial resolution fixed reduces the acquisition time by the same factor. This also decreases the field of view (FOV), resulting in aliasing or wrap-around artifact. In parallel imaging, the spatial dependence of the phased-array coil elements is used to remove or prevent the aliasing.

Simultaneous acquisition of spatial harmonics (SMASH), described by Sodickson and Manning (6), uses the sensitivity profiles as basis sets to generate spatial harmonics and eventually reconstruct the image in the Fourier domain; in other words, the missing k-space lines are restored prior to the Fourier transform. Generalized autocalibrating partially parallel acquisition (GRAPPA) is a variant of SMASH in which a small number of additional lines of k-space are acquired during the acquisition, eliminating the need for a separate coil sensitivity calibration acquisition (7). The GRAPPA reconstruction algorithm also provides improvements in SNR and elimination of certain artifacts relative to SMASH. Pruessmann et al (8) described an alternative image-based parallel imaging reconstruction (sensitivity encoding [SENSE]). In this method, the data are first Fourier transformed, resulting in aliased images. The images are then “unwrapped” by using the spatial information from the coil sensitivity profiles.

Since the introduction of parallel imaging, a number of different reconstruction techniques and strategies have been introduced; however, the most widely available techniques include SENSE, mSENSE (an autocalibrating version of SENSE), and GRAPPA. In the next section, a basic explanation of image-based parallel imaging (SENSE) is presented, followed by a brief discussion of the advantages and disadvantages of the image-based and k-space-based techniques.

### Theory

Image formation in MR imaging is based on the traversal of k-space in two or three dimensions in a manner determined by the pulse sequence. Although acquisition of data in the frequency-encoding direction is typically rapid and on the order of several milliseconds, a separate echo collected with a slightly different value of the applied phase-encoding gradient is required to sample each value of  $k_y$  along the phase-encoding axis. The sampling of k-space through a prescribed number of phase-encoding steps therefore accounts for the majority of the acquisition time in most MR imaging acquisitions.

The development of parallel imaging is motivated by the need to shorten acquisition time, typically through the undersampling of k-space along the phase-encoding direction (1–13). Generally, the number of sampled phase-encoding views is reduced by an acceleration factor  $R$ , thereby shortening the acquisition time by the same factor. For example, when  $R = 2$ , every other phase-encoding view, or only half of k-space, is sampled. As a result, the acquisition time is shortened by a factor of two. When  $R = 3$ , only a third of k-space is sampled and the acquisition time is reduced threefold. According to the SENSE algorithm,  $R$  can theoretically assume values up to the number of elements employed in the phased-array coil. In practice, however, most MR imaging vendors use  $R$  values ranging from 1.5 to 3, whereas the number of coil elements varies from four to 12.

Two parameters are of particular interest when implementing SENSE. First, the range of sampled values along the  $k_y$  axis ( $k_{y\text{-max}}$ ) determines the spatial resolution along the phase-encoding direction. As the total number of sampled views ( $N_y$ ) increases, higher k-space spatial frequencies are acquired, resulting in improved spatial

resolution along the phase-encoding axis. Second, the separation between successive views along the  $k_y$  axis ( $\Delta k_y$ ) determines the corresponding FOV ( $\text{FOV}_y$ ) in the image domain. When the SENSE algorithm is applied to reduce acquisition time, the number of sampled phase-encoding views ( $N_y$ ) is reduced by  $R$  ( $N_y/R$ ), whereas the maximal sampled values of  $k_y$  ( $k_{y\text{-max}}$ ) are not changed. This approach allows the SENSE-acquired image to have the same spatial resolution as the reference acquisition but at the expense of an increase in  $\Delta k_y$ . Owing to the inverse relationship between FOV and  $\Delta k_y$  (Eq [1]),

$$\Delta k_y = 1/\text{FOV}_y, \quad (1)$$

the resultant FOV along the phase-encoding axis in the SENSE acquisition is also reduced by  $R$ .

The consequent reduction in phase FOV with the SENSE technique typically introduces aliasing or wraparound artifacts in the raw Fourier transformed images. The SENSE reconstruction algorithm addresses this problem by using spatial information available from another source: individual elements from the phased-array surface coil assembly. Normally, the signals received from each phased-array element are summed to generate a composite image with improved SNR. In SENSE, the spatial sensitivity profile of each individual element is exploited to restore the original FOV.

The signal strength at a particular point varies as a function of the distance from the receiver coil. In theory, if the sensitivity profile of each coil element in the phased array can be obtained, then the signal intensity differences between each element at any given pixel in an image can be related to the spatial location of that point. This relationship in turn is used in the SENSE technique to unfold and remove the aliased artifacts from the raw SENSE-acquired images. The principal basis of SENSE is therefore to undersample k-space by using a reduced FOV and a smaller number of phase-encoding views, which typically introduces wraparound artifacts in the raw images, but to use previously calibrated coil sensitivity maps to account for this in the reconstruction.

The SENSE algorithm has been previously explained in detail in the literature (8–10). A simplified schematic of the method is shown in Figure 1 for  $R = 2$ . In Figure 1a, a reference full-FOV non-SENSE image from the body receiver coil is shown. In Figure 1b, the same image is shown as the sum-of-squares from two individual coil elements, which are placed above and below the object along the y axis. A corresponding reference k-space containing a total of 20 phase-encoding views is also shown for illustration simplicity. The image has not been intensity corrected to illustrate the heterogeneous distribution of signal intensity across the object. Spins at spatial locations closer to the coil elements exhibit higher signal levels than those that are farther away.

The SENSE implementation begins with Figures 1c and 1d. First, low-resolution full-FOV images are obtained to calculate the complex sensitivity profiles of each coil element. Second, the reduced-FOV SENSE acquisition is performed. This leads to raw images from each of the coil elements with extensive wraparound artifacts along the superior-to-inferior phase-encoding axis (Figure 1e, 1f). Using the previously measured complex sensitivity data, the reconstruction algorithm unfolds the aliased images by solving a set of linear equations to determine true pixel values in the desired full-FOV image. These equations represent the relationship that each wraparound data point  $[a]$  in the aliased images is the result of a linear superposition of unaliased pixels  $[p]$ , correspondingly weighted by the sensitivities  $[s]$  of each coil element at each spatial location.

Since  $[a]$  and  $[s]$  are known from separate acquisitions and  $[p]$ , as shown in Figure 1g, effectively represents the desired unaliased image, a unique solution to  $[p]$  can be determined through mathematical formulation. By adopting the symbols of Figure 1c–1f, an equation relating  $[a]$ ,  $[s]$ , and  $[p]$  can be formed for each coil element:

For coil 1,

$$a_1 = s_{1,1} \cdot p_1 + s_{1,2} \cdot p_2. \quad (2a)$$

For coil 2,

$$a_2 = s_{2,1} \cdot p_1 + s_{2,2} \cdot p_2. \quad (2b)$$

In Equation (2),  $R = 2$ ,  $p_1$  and  $p_2$  denote the unknown pixel values that are to be determined, and two independent equations have been formed from two coil elements. For simplification, Equations (2a) and (2b) can be written in matrix form:

$$[a] = [s] \cdot [p]. \quad (3)$$

Subsequently, a unique solution to the desired full-FOV image  $[p]$  can be determined with the following formula:

$$[s]^{-1}[a] = [p], \quad (4)$$

where  $[s]^{-1}$  represents the inverse matrix of  $[s]$ .

To properly reconstruct the SENSE image, Equation (4) must be performed for every pixel in the aliased image set. Figures 1h and 1i illustrate the SENSE-reconstructed image and the corresponding intensity-corrected result. Compared to the reference images shown in Figures 1a and 1b, the reconstructed SENSE images exhibit similar quality in terms of contrast and spatial resolution (but reduced SNR) while having been obtained in only half the acquisition time.

In principle, the SENSE reduction factor  $R$  can be as large as the total number of phased-array coil elements in determining a unique solution to  $[p]$ . In practice, however, many vendors implement parallel imaging with an  $R$  factor much smaller than the number of available coil elements, partly to allow a robust and solid solution to  $[p]$ . There are also practical limitations to the maximum reduction factor in parallel imaging, and these restrictions have thus far prevented the widespread application of SENSE with  $R$  factors greater than 2–3. For example, in cases where SENSE is implemented to reduce acquisition time, as  $R$  increases, the SNR of the image diminishes with the following relationship:

$$\text{SNR} \approx 1/(g \cdot R^{1/2}), \quad (5)$$

where  $g$  is defined as a factor dependent on coil geometry and is a measure of how well a particular coil arrangement can unwrap a particular aliasing pattern. The geometry factor depends on the distinctness or independence of each coil element's sensitivity behavior over the aliased pixels. In addition to coil properties such as positioning and decoupling that affect the sensitivity behavior, the geometry factor also depends on the

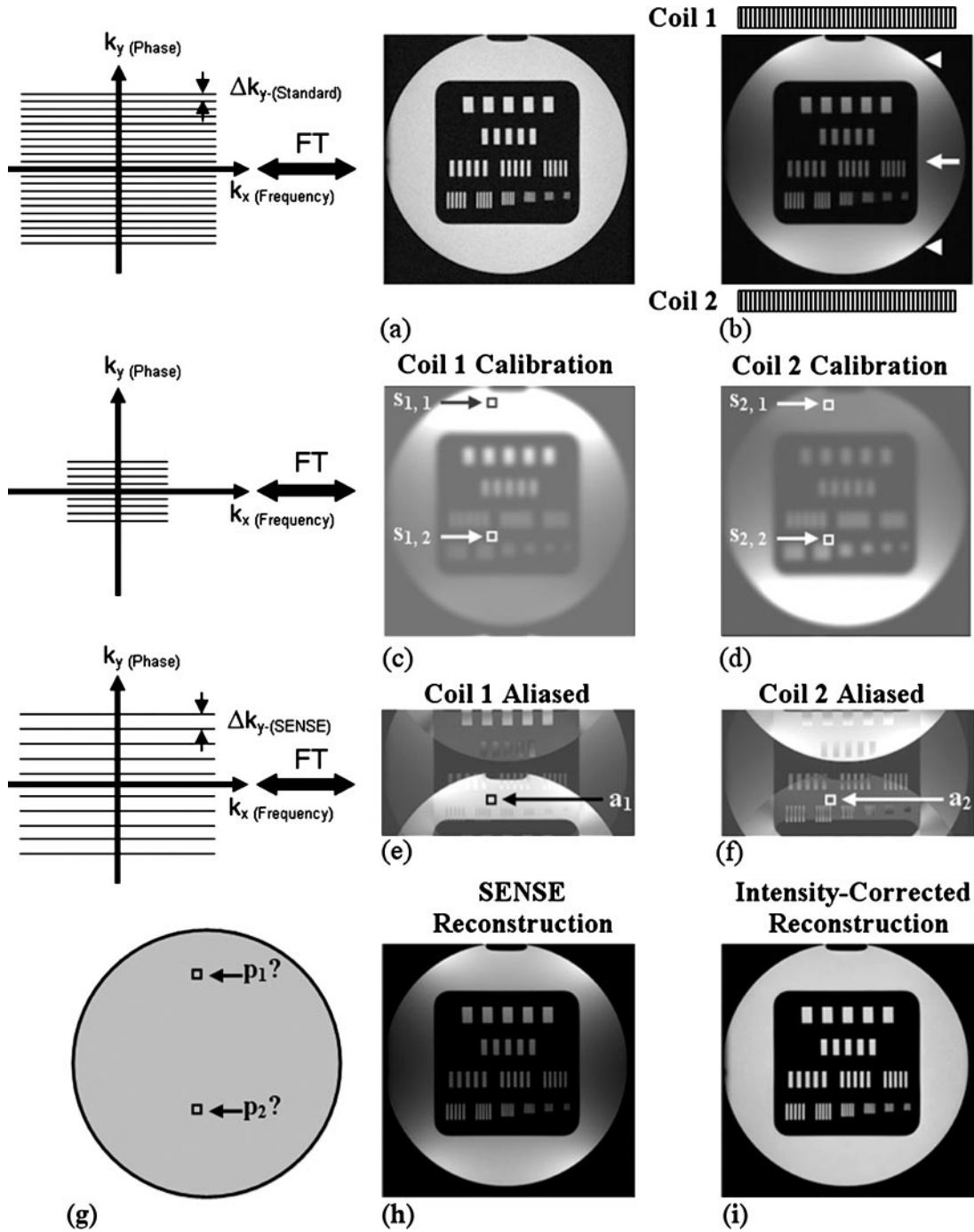


**Figure 1.** Example of the SENSE technique. Reference image of a phantom (a), obtained with the body receiver coil. Sum-of-squares image (b) from two individual coil elements. Spins at spatial locations closer to the coil elements (arrowheads) exhibit higher signal levels than those that are farther away (arrow). A corresponding reference k-space containing 20 phase-encoding views is shown at left. *FT* = Fourier transform. Low-resolution full-FOV calibration images (c and d) for each coil, which were obtained to calculate the complex sensitivity profiles of each coil element. Sensitivities ( $s_1$  and  $s_2$ ) of each coil element are illustrated at two arbitrary points. Reduced-FOV SENSE images (e and f) from each coil element contain extensive wraparound artifacts along the superior-to-inferior phase-encoding axis.  $a_1$  and  $a_2$  represent the signal intensities of the aliased images that correspond to the arbitrary points chosen in c and d. Diagram of the unaliased image (g) with desired pixel intensities  $p_1$  and  $p_2$ . These intensities can be calculated because the sensitivities of the individual coil elements and the pixel intensities of the aliased images are known. Unaliased image without (h) and with (i) intensity correction, which represents the SENSE-reconstructed image.



**Parallel Imaging Terms and Vendor Acronyms**

Term	Acronym	Vendor
Sensitivity encoding	SENSE	Philips Medical Systems*
Array spatial sensitivity encoding technique	ASSET	GE Healthcare Technologies <sup>†</sup>
Integrated parallel acquisition techniques	IPAT	Siemens Medical Solutions <sup>‡</sup>
Generalized autocalibrating partially parallel acquisition	GRAPPA	Siemens Medical Solutions
Simultaneous acquisition of spatial harmonics	SMASH	...

\*Best, the Netherlands.

<sup>†</sup>Waukesha, Wis.

<sup>‡</sup>Erlangen, Germany.

imaging plane, FOV, reduction factor, and phase-encoding direction.

Reduction in SNR can become critical for large acceleration factors, particularly for pulse sequences that are inherently low in signal. In addition, as  $R$  increases, the aliasing artifacts occur to a greater degree as the raw SENSE image is folded over an increasing number of times along the phase-encoding axis. With greater  $R$ , errors in the sensitivity measurement are more detrimental, resulting in more uncorrected aliasing. Consequently, the determination of a solution to the inverse matrix problem in Equation (4) becomes more difficult. In practice, because of errors in alias unwrapping and because of noise magnification by the geometry factor,  $R$  is limited by the number of coils separated in the phase-encoding direction rather than the total number of coils.

Coil positioning and placement about the imaging object is also a critical factor in successful implementation of SENSE. In the ideal situation, it is desired that coil elements not only behave independently but also have the highest spatial sensitivity gradient along the direction in which SENSE reconstruction is applied. For example, if the phase-encoding direction is anterior to posterior, it is more effective to position the coil elements on the anterior and posterior surfaces of the patient rather than on the right and left. Coil positioning and geometry become particularly important, and more complex, when SENSE is applied along two phase-encoding directions in three-dimensional (3D) MR imaging acquisitions. For a given acquisition time (given total  $R$ ), smaller reductions can be used in both Fourier encoding directions for the 3D case than are needed to achieve the same total  $R$  in a single direction for the two-dimensional (2D) case. Since the geometry factor increases rapidly with increasing  $R$ , parallel imaging along two directions can

have a lower overall geometry factor for the same total  $R$ . Many existing coils do not have element orientation appropriate for parallel imaging in two directions. This is one reason that many vendors are currently designing coils specifically optimized for parallel imaging.

A number of vendor-specific acronyms have appeared regarding application of parallel imaging. These are summarized in the Table. Although demonstrated by using SENSE parallel imaging, the application benefits shown in this article can be realized with all parallel imaging techniques.

### Calibration Acquisitions

Many applications of parallel imaging involve a separate calibration acquisition. This is a fast, low-resolution acquisition (typically a fast gradient-echo sequence) that is subsequently used to map the spatial sensitivity of each phased-array element. For breath-hold applications of parallel imaging, the calibration acquisition should also be performed with suspended respiration. The calibration acquisition can be performed in any plane orientation and should encompass all regions that will be covered in the parallel imaging acquisition. A large FOV is used to prevent aliasing in the calibration acquisition, which will introduce errors in the reconstruction. The calibration acquisition can be included within the parallel imaging acquisition (autocalibration, self-calibration, GRAPPA); however, this results in slightly longer acquisition times.

### Choosing the Optimal Parallel Imaging Method

Currently, the choice of the optimal parallel imaging technique is limited to a certain extent by commercial availability. Some vendors offer one method, whereas others offer two or more options, although the number of available techniques will undoubtedly increase in the near future. The choice between a self-calibrating

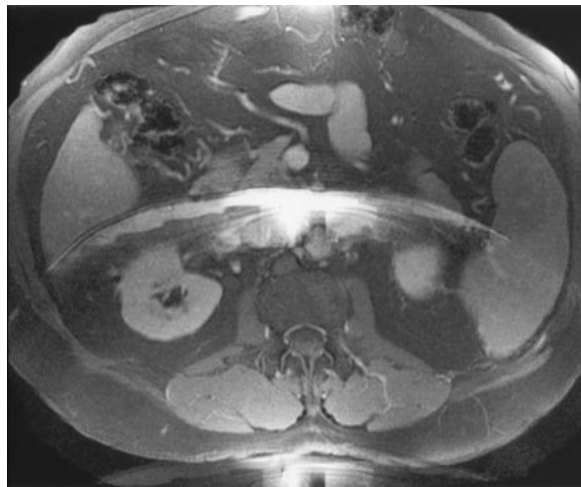


**Figure 2.** Axial contrast-enhanced 2D spoiled gradient-echo (SPGR) image obtained with SENSE (acceleration factor = 2, applied in the anteroposterior phase-encoding direction) shows extensive artifact in the center of the image due to uncorrected aliasing. This artifact could be reduced by increasing the FOV in the anteroposterior direction.

k-space technique such as GRAPPA and the image-domain SENSE requiring a separate calibration acquisition can rest on a number of factors. If speed is the paramount concern, then the addition of extra self-calibration k-space lines may be disadvantageous, and SENSE might be the best choice. This is a more crucial concern for relatively low-resolution images: As the image matrix increases, the self-calibration lines of k-space occupy a smaller percentage of the total acquisition time. A second advantage of SENSE is that in general it provides slightly better image quality with high acceleration factors.

On the other hand, there are situations where GRAPPA may be the preferred technique. In regions where accurate coil sensitivity maps are difficult to obtain (eg, the lungs), the GRAPPA algorithm may provide a more robust reconstruction. In breath-hold applications of parallel imaging, some patients may have difficulty suspending respiration in a reproducible manner, leading to discrepancies between the calibration acquisition and the parallel imaging acquisition, which in turn can result in reconstruction artifacts. In this case the autocalibration technique may be preferred, but only if the acquisition time remains within the patient's breath-hold capacity.

A second advantage of GRAPPA has to do with the imaging FOV. In SENSE-like image-based techniques, if the full FOV is smaller than the object, artifacts can be generated in the reconstructed image. The solution is to ensure that

there is no aliasing in the reconstructed image. On the other hand, GRAPPA is able to generate partially aliased reconstructed images without significant artifact, so that a smaller FOV can be chosen when spatial resolution is an important consideration.

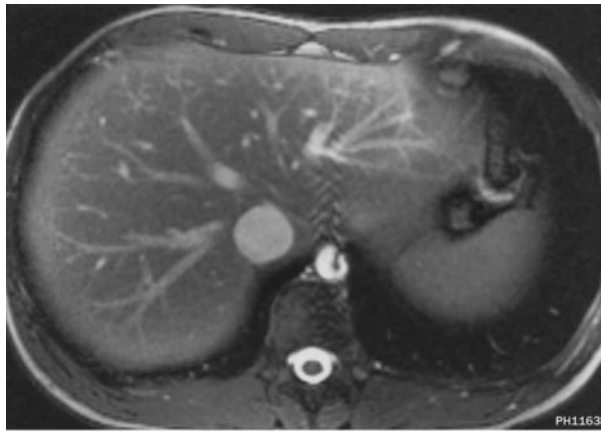
### Artifacts

A number of artifacts can be encountered in parallel imaging. Many of these can be eliminated with careful attention to technique; however, some are unavoidable. Ghosting artifacts may appear when the calibration acquisition and parallel imaging acquisition are not performed with the patient in the same position. This can occur if the calibration acquisition was not performed during suspended respiration or if the breath-holding position was different between the two acquisitions. This problem can be eliminated with techniques that include the calibration acquisition in the parallel imaging acquisition, at the cost of a slight increase in acquisition time. If the calibration acquisition does not include a region that is subsequently imaged in the parallel acquisition, this region cannot be reconstructed, and a void will appear in the image.

Another result of inadequate calibration volume coverage is uncorrected aliasing that arises from locations outside the calibration volume that alias into the calibrated locations. This problem can occur with highly oblique planes, for example in cardiac imaging with short-axis acquisitions. This can be remedied by including all regions covered by the coil in the calibration acquisition. Poorly positioned calibration acquisitions may generate aliasing within the calibration acquisition that will cause additional artifact in the reconstructed images. Careful centering of calibration acquisitions and use of a large FOV will generally eliminate this artifact.

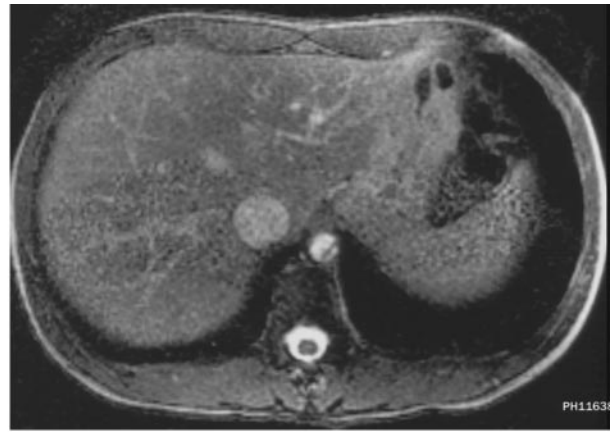
Artifacts may also appear when the FOV is too small in the parallel acquisition. When this occurs, uncorrected aliasing artifacts may arise from structures separated by the aliasing distance in the phase-encoding direction (eg, half the FOV for the  $R = 2$  case). Unfortunately, this often has the effect of placing wraparound artifact at or near the center of the image (Fig 2). This can be corrected by increasing the FOV so that no aliasing will appear in the reconstructed image.

Finally, artifacts can appear in regions of low SNR, for example, in the center of a large patient

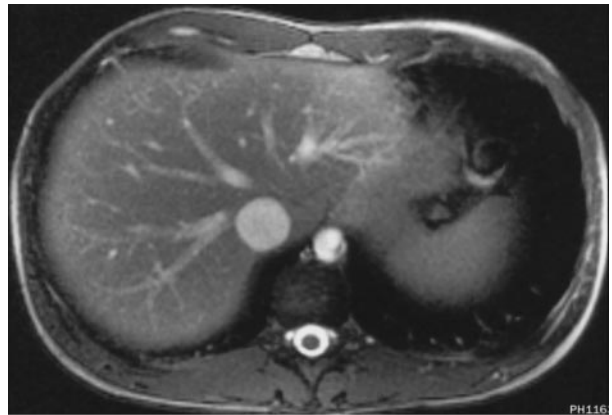


a.

**Figure 3.** (a) Standard axial 2D steady-state free precession image of the liver. (b) SENSE image (acceleration factor = 2, applied in the anteroposterior phase-encoding direction) obtained with the same FOV as in a. Noise and reconstruction artifacts in the middle of the FOV limit the diagnostic quality of the image. (c) SENSE image (acceleration factor = 2) obtained with an increased phase FOV in the anteroposterior direction shows that the artifacts have been eliminated. Note that the phase ghosting artifact due to aortic pulsation in the standard image has been significantly reduced in the SENSE images.



b.



c.

relatively distant from any surface coil (Fig 3). Noise in parallel imaging is not evenly distributed, and in regions of suboptimal coil geometries (ie, high  $g$  factors) it may be amplified. These artifacts can be reduced to a certain extent by maximizing achievable SNR; however, some artifacts may be unavoidable in these cases, particularly when high  $R$  values are applied.

### Clinical Applications

One of the most important advantages of parallel imaging is its wide applicability: Parallel imaging can be applied to nearly any pulse sequence, and the gains in acquisition speed can be used in a number of different ways, as illustrated in the following sections.

### MR Angiography

Contrast-enhanced 3D MR angiography has become the standard technique for body and peripheral MR angiography by virtue of its speed, high SNR, minimal artifacts, and relatively high spatial resolution. Nevertheless, examinations are not always ideal, and perhaps the most frequently encountered problem is an acquisition time that exceeds the patient's breath-hold capacity. Parallel imaging can directly address this by reducing the acquisition time by a factor of two or greater

(Fig 4) (12–19). Parallel imaging not only helps reduce motion artifact but can also diminish venous contamination, particularly in regions where there is rapid venous return, such as the renal and carotid arteries (20) (Fig 5).

Venous contamination is also a frequent problem in lower extremity runoff examinations. Imaging the upper stations is relatively time-consuming; when the most distal station is reached, the acquisition may be far enough behind the contrast material bolus that venous contamination is seen. Parallel imaging has been used at one or more of the upper stations to ensure that the most distal station is reached quickly enough to minimize venous contamination (15). In one study (19), it was noted that SNR and contrast-to-noise ratio were actually improved at stations where SENSE was used. The explanation for this is not entirely certain but may be related to the ability to inject contrast material at a higher rate or to capture the first pass of the contrast material bolus more efficiently.

By combining higher acceleration factors with lower spatial resolution, time-resolved MR angiography can be performed with temporal resolution on the order of a few seconds. This can be useful for resolving flow dynamics through a par-



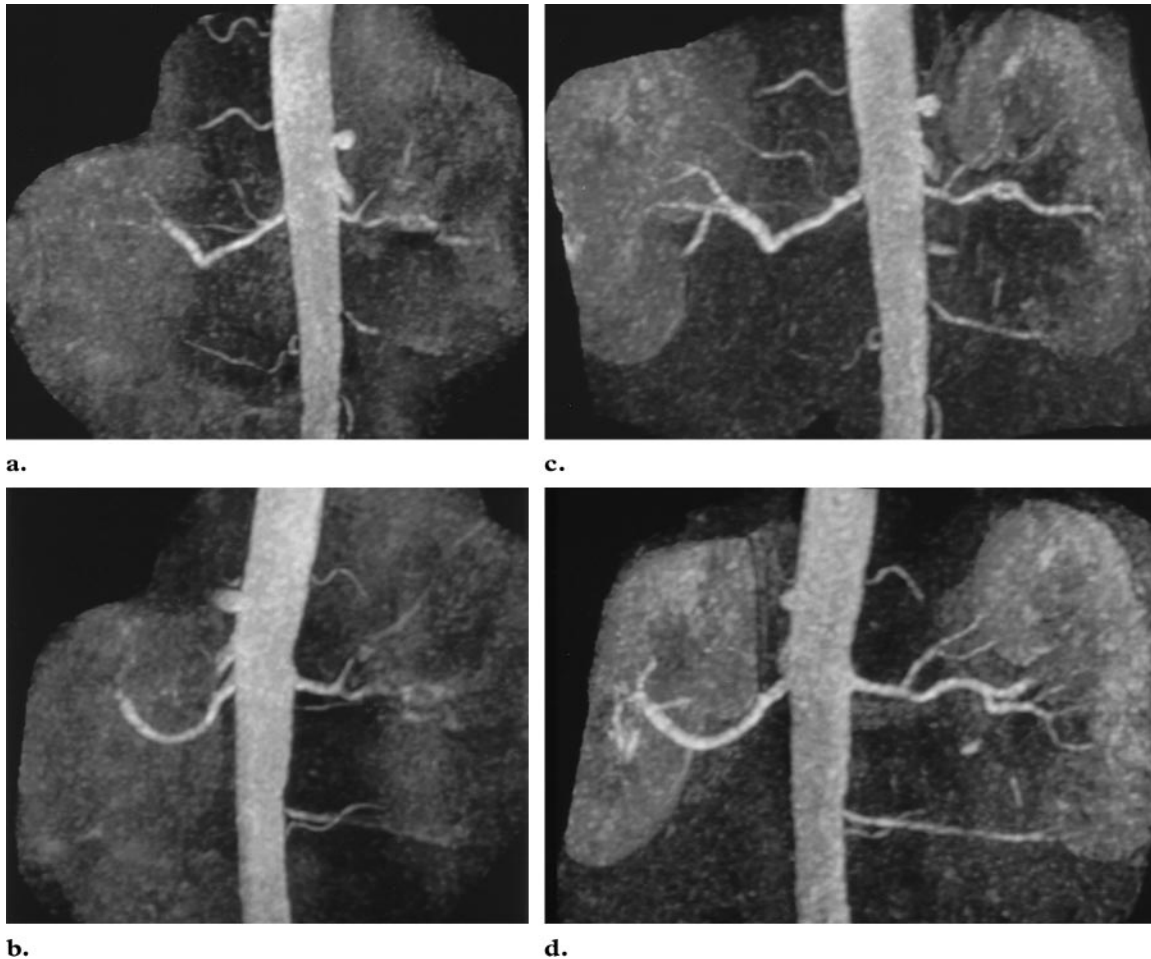


**Figure 4.** Partial volume maximum intensity projection images from 3D contrast-enhanced renal MR angiography. The images were obtained in the right (**a, c**) and left (**b, d**) lateral oblique projections without (**a, b**) and with (**c, d**) SENSE (acceleration factor = 2, applied in the in-plane right-left phase-encoding direction). Note the improved visualization of segmental renal arteries in the SENSE images. The patient was short of breath and had difficulty suspending respiration for the standard acquisition time. Parallel imaging was used to reduce the acquisition time from 19 seconds to 10 seconds.

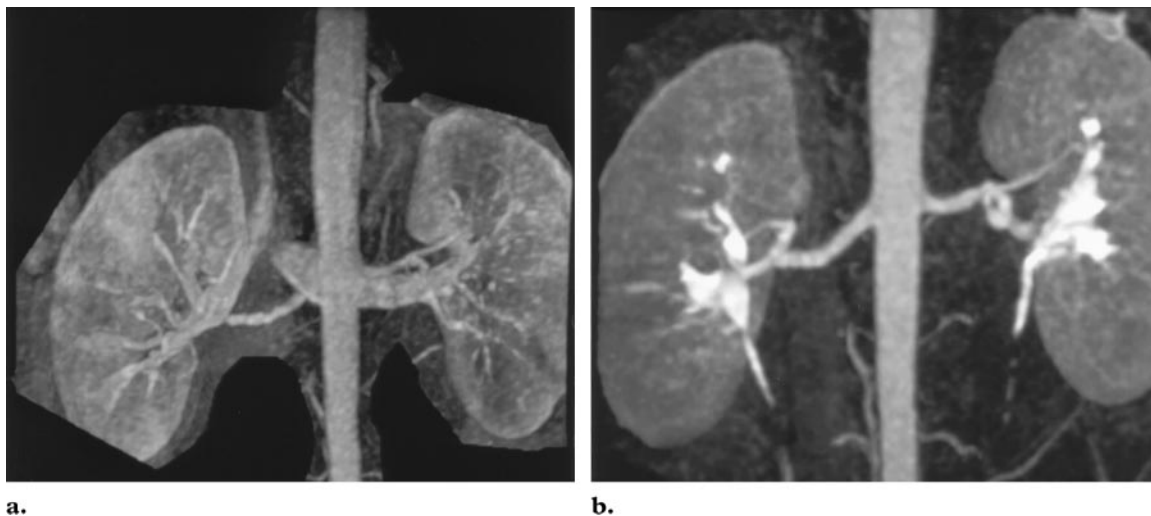


**Figure 5.** Partial volume maximum intensity projection images from renal MR angiography of a patient with fibromuscular dysplasia, obtained without (**a**) and with (**b**) SENSE (acceleration factor = 2, applied in the in-plane right-left phase-encoding direction). In the standard image, early filling of the left renal vein limits visualization of the left renal artery. Venous contamination is eliminated in the SENSE image, which was obtained with the acquisition time reduced by half. Collecting system activity in the SENSE image is due to excretion of contrast material from the first non-SENSE acquisition.

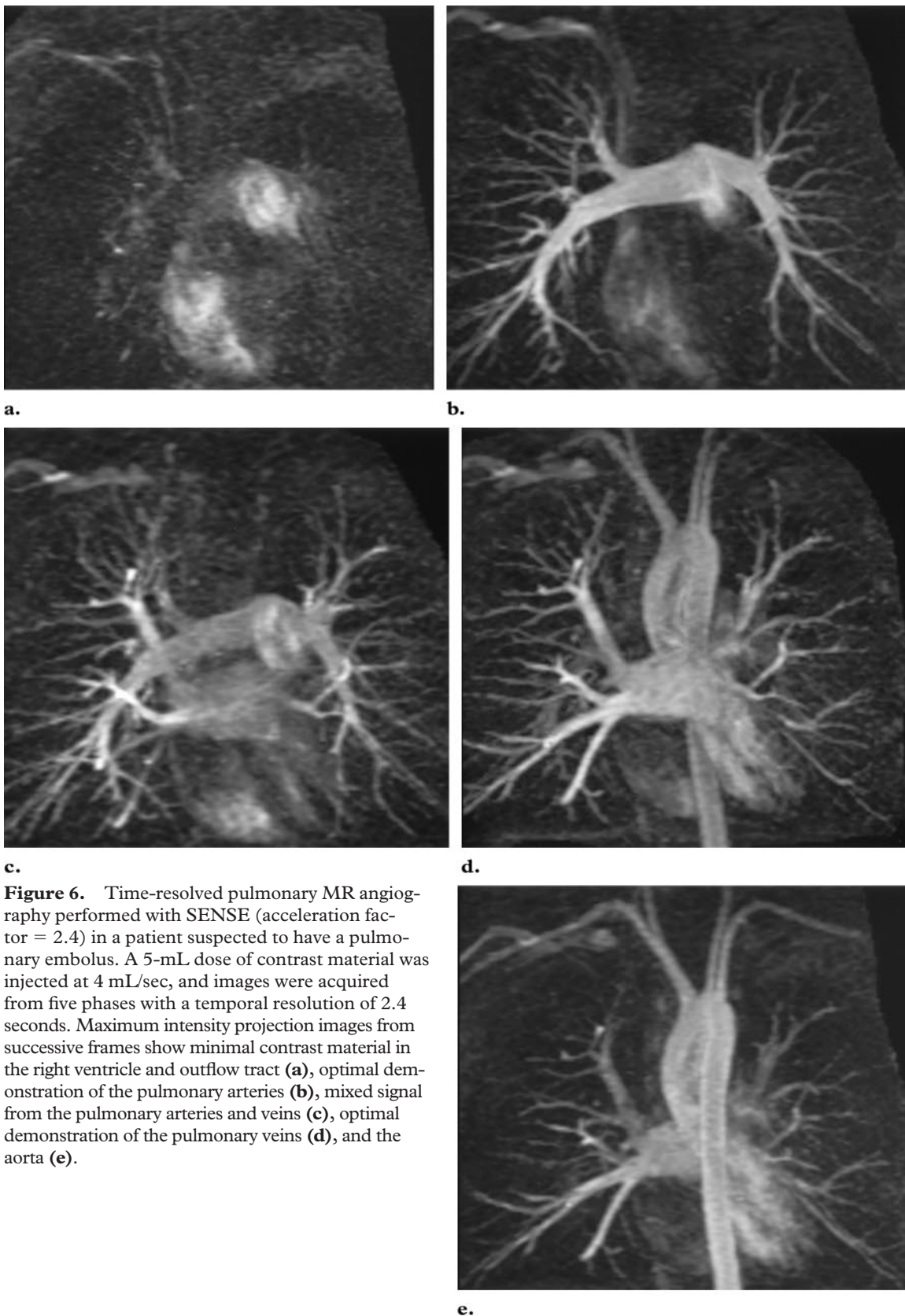


**Figure 6.** Time-resolved pulmonary MR angiography performed with SENSE (acceleration factor = 2.4) in a patient suspected to have a pulmonary embolus. A 5-mL dose of contrast material was injected at 4 mL/sec, and images were acquired from five phases with a temporal resolution of 2.4 seconds. Maximum intensity projection images from successive frames show minimal contrast material in the right ventricle and outflow tract (**a**), optimal demonstration of the pulmonary arteries (**b**), mixed signal from the pulmonary arteries and veins (**c**), optimal demonstration of the pulmonary veins (**d**), and the aorta (**e**).



**Figure 7.** Image from 3D contrast-enhanced MR angiography of the abdominal aorta performed with SENSE (acceleration factor = 2, applied in the in-plane right-left direction) to improve spatial resolution. Forty 1.6-mm-thick sections were obtained in 21 seconds with an in-plane matrix of  $320 \times 256$  and a 32-cm FOV, yielding a high spatial resolution of  $1.0 \times 1.25 \times 1.6$  mm.

ticular vascular territory (Fig 6) (16–18) and also is an alternative technique to standard MR angiography in patients who are very short of breath.

The gains in speed achieved with parallel imaging can alternatively be applied to improve spatial resolution. If the acquisition time is kept constant, additional phase-encoding steps can be acquired, thereby increasing resolution in the phase-encoding direction (Fig 7). However, the combination of parallel imaging and increased spatial resolution will usually result in a significant reduction in SNR. Therefore, it is important to ascertain that the signal intensity is high enough in the reconstructed images to achieve a diagnostic examination.

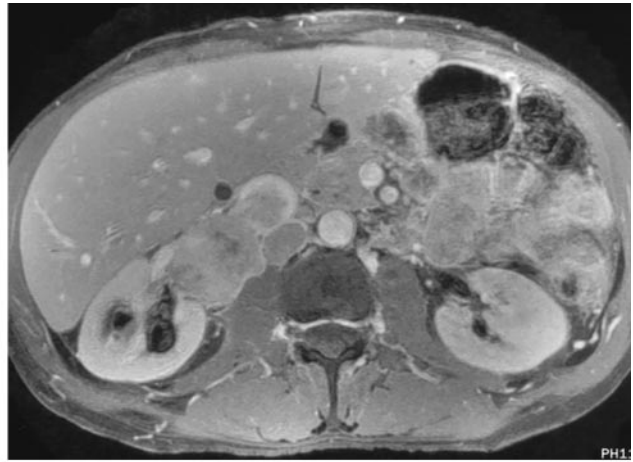
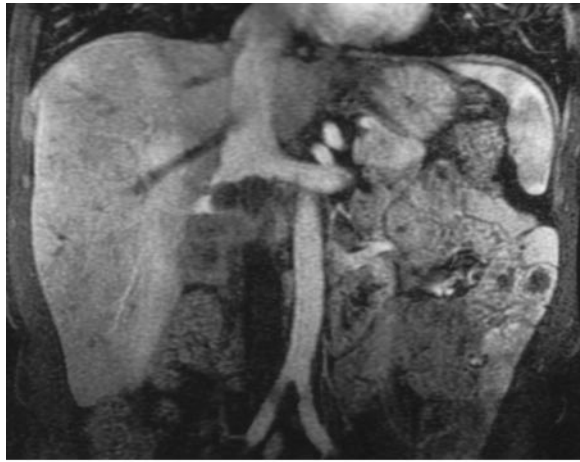
The latter problem can be alleviated by careful attention to maximizing SNR. This includes use of eight-, 12-, 16-, and 32-channel coils, positioning the patient so that the region of interest is in the center of the phased-array coil, and optimizing imaging parameters in the MR angiography sequence. (Unfortunately, most of the choices leading to higher SNR also increase the acquisition time.) If the application of parallel imaging results in a reduced acquisition time, the contrast

material injection rate can be increased, since the optimal length of the bolus injection is related to the acquisition time. By injecting the same volume of contrast material more quickly, a higher intraarterial first-pass concentration can be achieved, resulting in increased signal intensity. This approach may alleviate some of the SNR reduction caused by the application of parallel imaging. Another approach to the SNR problem is to image at higher magnetic field strengths; 3-T clinical systems have recently been introduced by most vendors, and several authors have demonstrated that MR angiography is particularly suited to this environment (21,22). The combination of 3-T imaging and parallel imaging techniques is therefore very attractive and may become a common clinical technique in the future.

Alternatives to 3D contrast-enhanced MR angiography may also benefit from parallel imaging. Time-of-flight techniques are of limited value in the chest and abdomen because the long acquisition times preclude breath-hold imaging. This can be alleviated to some extent with parallel imaging. Phase-contrast sequences are also limited by relatively long acquisition times, which can similarly be reduced by the application of parallel imaging. For example, cardiac-gated cine phase-contrast sequences are useful in a number of clinical situations to quantify velocity or blood flow. In most thoracic and abdominal applications, acquisitions during suspended respiration are desirable because they allow accurate tracing of vessel borders free from respiratory motion artifact.

To achieve acquisition during suspended respiration, most breath-hold cine phase-contrast sequences employ a segmented k-space acquisition scheme in which a number of k-space lines, or views per segment, are sampled for each phase of the cardiac cycle every heartbeat. As the number of views per segment increases, the acquisition time shortens but the temporal resolution of velocity sampling is reduced, and this may limit the accuracy of measurements in regions of rapidly varying velocity and flow. By reducing the total number of sampled k-space lines, parallel imaging offers additional freedom in balancing the demands of relatively short acquisition times and adequate temporal resolution. Steady-state free precession sequences have been used as a nonenhanced bright-blood vascular technique; this





a.

b.

**Figure 9.** Contrast-enhanced fat-saturated SPGR imaging performed with SENSE (acceleration factor = 2) in a patient with a renal cell carcinoma invading the right renal vein and inferior vena cava. **(a)** Coronal early venous phase 3D image. Sixty 3-mm-thick sections with a  $256 \times 224$  matrix were obtained in 18 seconds. **(b)** Axial 2D image. SENSE was used to improve the spatial resolution ( $320 \times 256$  matrix) with only minimally increased acquisition time.

method in combination with parallel imaging is particularly effective for very rapid screening of large veins or arteries in patients who are short of breath or incapable of suspending respiration (Fig 8).

### Dynamic Contrast-enhanced Imaging

Contrast-enhanced 2D and 3D fat-saturated SPGR sequences are commonly used to identify and characterize parenchymal lesions in the liver, kidneys, pancreas, and other organs. Achieving complete coverage with adequate temporal and spatial resolution can be challenging at times; this is particularly true for lesions that enhance in the arterial phase and rapidly wash out, such as small hepatocellular carcinomas, focal nodular hyperplasia, and certain metastatic lesions. Parallel imaging can be used to reduce acquisition times, thereby optimizing the length of the arterial phase and minimizing motion artifact from poor breath holding. Alternatively, spatial coverage can be increased in the same acquisition time or spatial resolution can be improved (Figs 9–11) (23,24).

### Fast SE Imaging

Fast SE, single-shot fast SE, and fast-recovery fast SE sequences are a mainstay of abdominal and pelvic imaging. Single-shot fast SE sequences

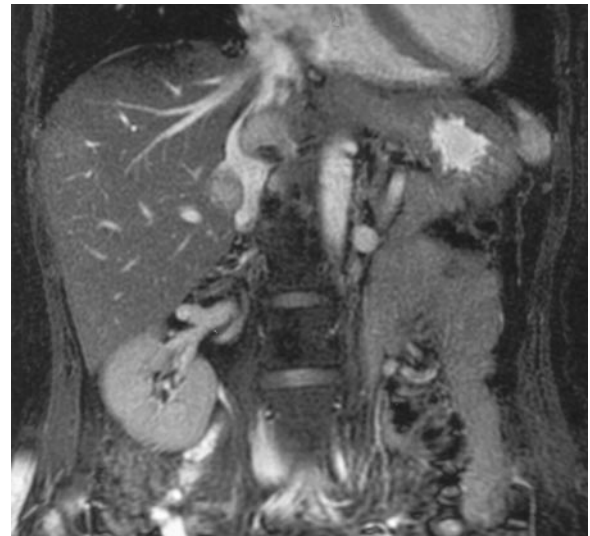


**Figure 8.** Coronal 2D fat-saturated steady-state free precession image of a patient with a metastatic pheochromocytoma, obtained with SENSE (acceleration factor = 2, applied in the in-plane right-left direction), shows metastases compressing the intrahepatic inferior vena cava. Twenty 2-mm-thick sections with a  $224 \times 256$  matrix were obtained in a breath hold of 15 seconds.

are particularly useful for MR cholangiopancreatography but are occasionally limited by image blurring, which is caused by the long echo train length of these sequences (24,25). Parallel imaging, by acquiring only half or fewer of the usual number of phase-encoding steps, shortens the



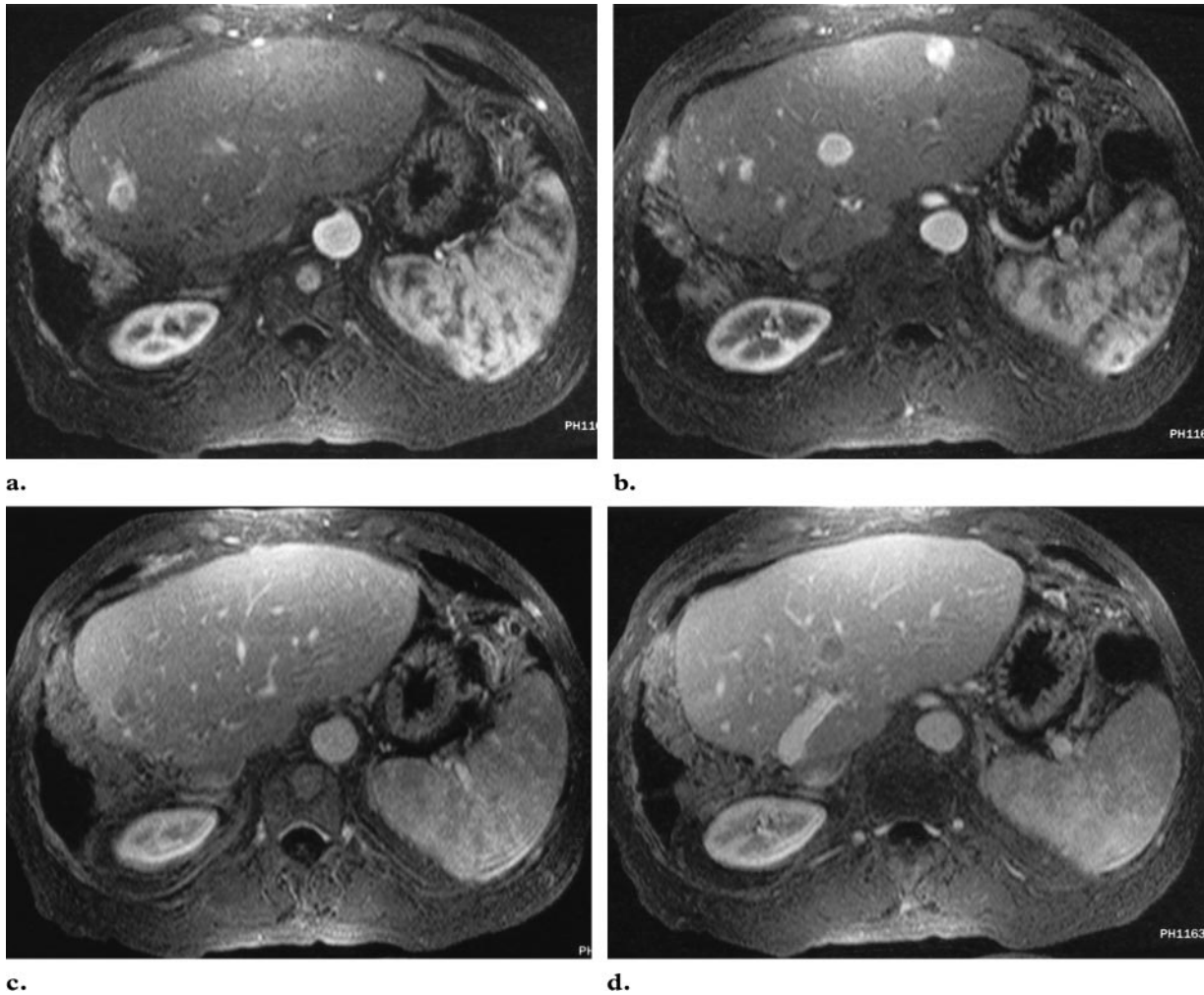


**Figure 10.** Axial arterial phase (**a, b**) and portal venous phase (**c, d**) fat-saturated 3D SPGR images of a patient with a metastatic neuroendocrine tumor. The images were obtained with SENSE (acceleration factor = 2, applied in the anteroposterior phase-encoding direction), with **a** and **c** acquired slightly superior to **b** and **d**. SENSE was used to achieve both excellent temporal and excellent spatial resolution. In this case, achieving optimal timing and adequate coverage in the arterial phase was crucial because many of the early enhancing hepatic and osseous metastases could not be visualized on images from subsequent phases.

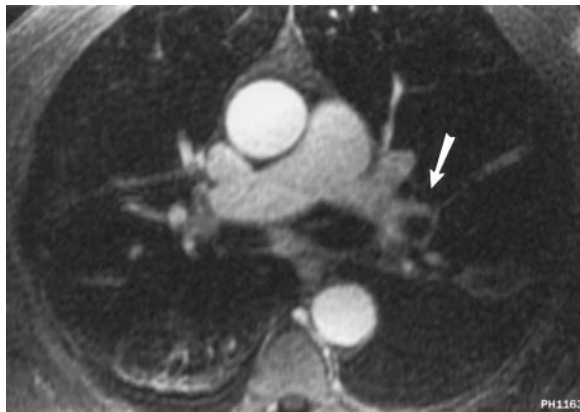
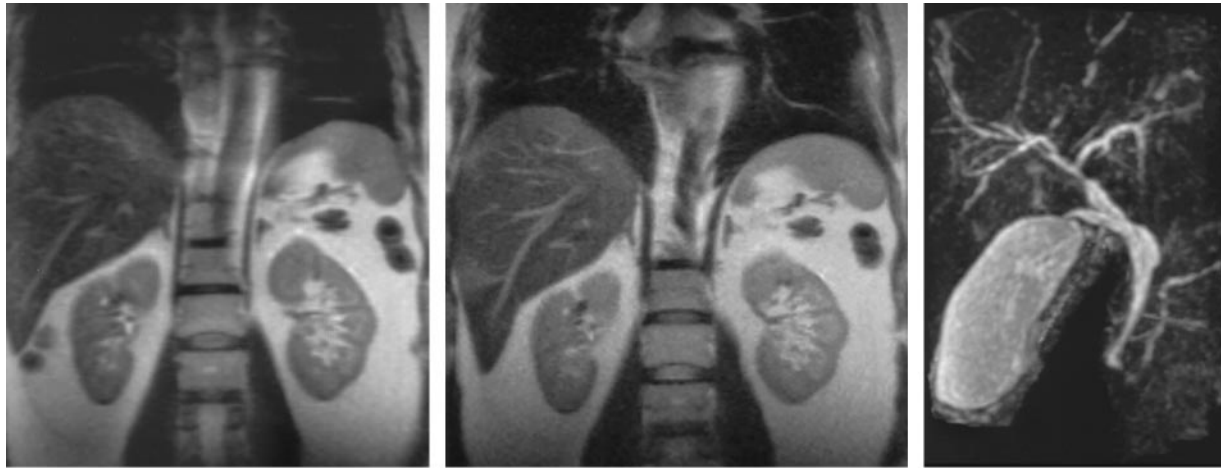


**Figure 11.** Axial contrast-enhanced fat-saturated 3D SPGR image of a patient with renal insufficiency who was suspected to have a pulmonary embolus. SENSE (acceleration factor = 2.2, applied in the anteroposterior in-plane phase-encoding direction) was used to reduce the acquisition time to 10 seconds because the patient was moderately short of breath. Note the large embolus in the left lower lobe segmental artery (arrow).



12a.

12b.

13.

**Figures 12, 13.** (12) Coronal single-shot fast SE image obtained without (a) and with (b) SENSE (acceleration factor = 2). Although the SENSE image has slightly diminished SNR, it also has slightly less blurring. (13) Maximum intensity projection image from 3D fast-recovery fast SE MR cholangiopancreatography. SENSE (acceleration factor = 2) was used to reduce the acquisition time sufficiently so that an adequate volume could be obtained within a comfortable breath hold.

echo train length significantly and thereby helps reduce image blurring (Fig 12). Parallel imaging also reduces the minimum repetition time (TR) for single-shot fast SE, fast SE, and fast-recovery fast SE sequences because the echo train length is reduced by a factor of two or more, and this in turn allows shorter acquisition times. The reduction in TR may not always be desired, but it is occasionally useful for sequences requiring suspended respiration that would otherwise have prohibitively long acquisition times (Fig 13).

Breath-hold fast SE and fast-recovery fast SE sequences are commonly used in hepatic imaging; however, it is generally conceded that the conspicuity of solid lesions is lower than that achieved with respiratory-triggered fast SE sequences. This is also at least in part related to the longer echo train lengths needed to achieve adequate coverage and spatial resolution within a breath hold. Parallel imaging can be used to reduce echo train lengths in these sequences without significantly increasing acquisition times and thereby may improve lesion conspicuity. The versatility of parallel imaging therefore allows a number of different

approaches to modifying standard fast SE sequences: reduction in the minimum TR, increased number of sections per acquisition at a fixed TR, improved spatial resolution for a fixed acquisition time, or even multiple signals averaged during a breath-hold acquisition (26).

### Cardiac Imaging

Cardiac MR imaging is particularly well-suited to the application of parallel imaging (9,27–31). Standard examinations generally consist of a large number of breath-hold acquisitions; this can be burdensome even under the best of circumstances and is especially problematic in patients with severe cardiac disease and shortness of breath. Parallel imaging can reduce the total number and/or length of breath holds required in an examination and thereby significantly reduce the total examination time. For example, complete coverage of the heart with short-axis cine steady-state free precession images can be achieved in three or four breath holds rather than 10–12 (Fig 14). In fact, the entire heart can be covered in a single breath hold by employing higher acceleration factors and making minimal compromises in spatial resolution. Black-blood double and triple inversion-recovery sequences likewise have high SNR and

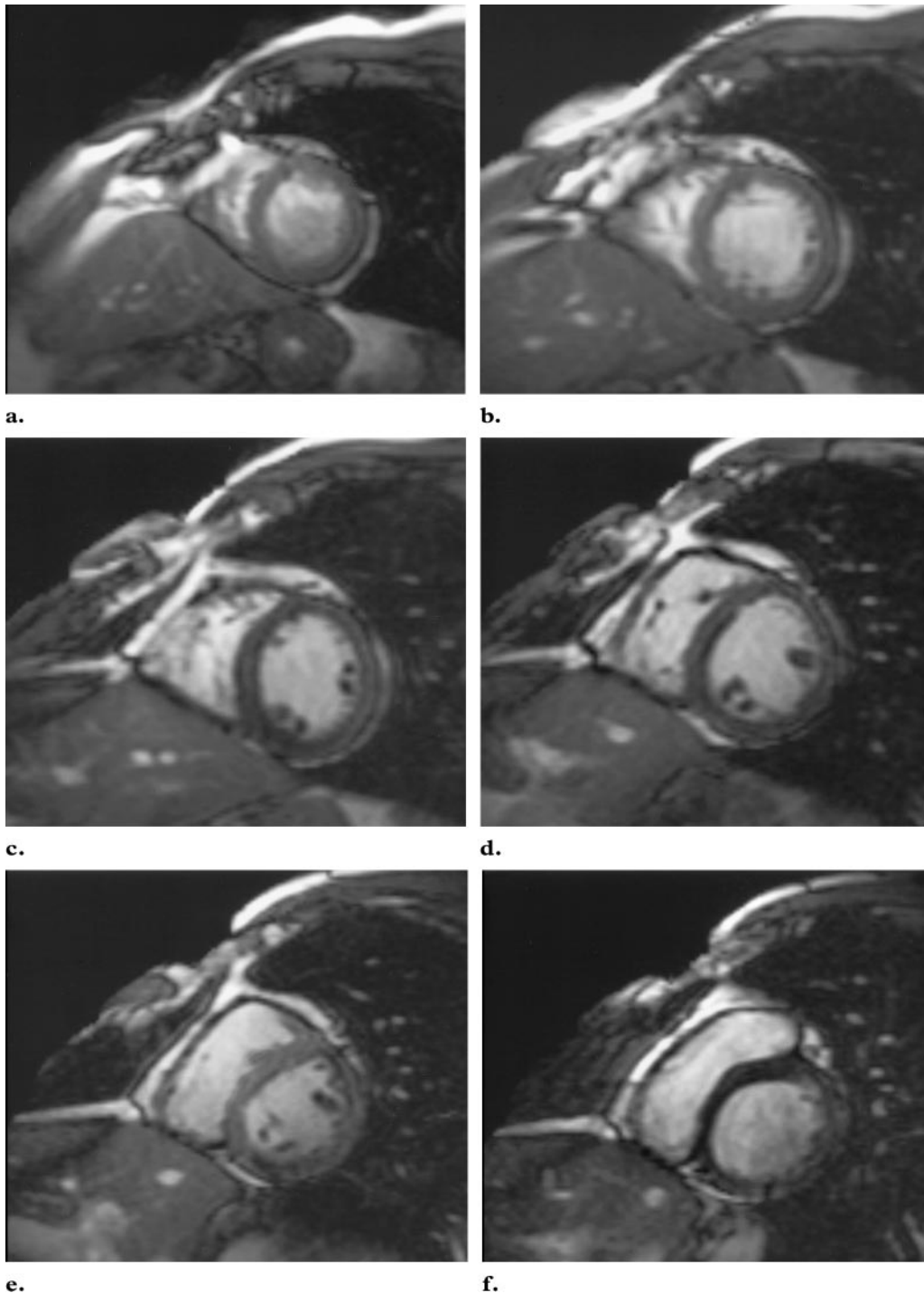
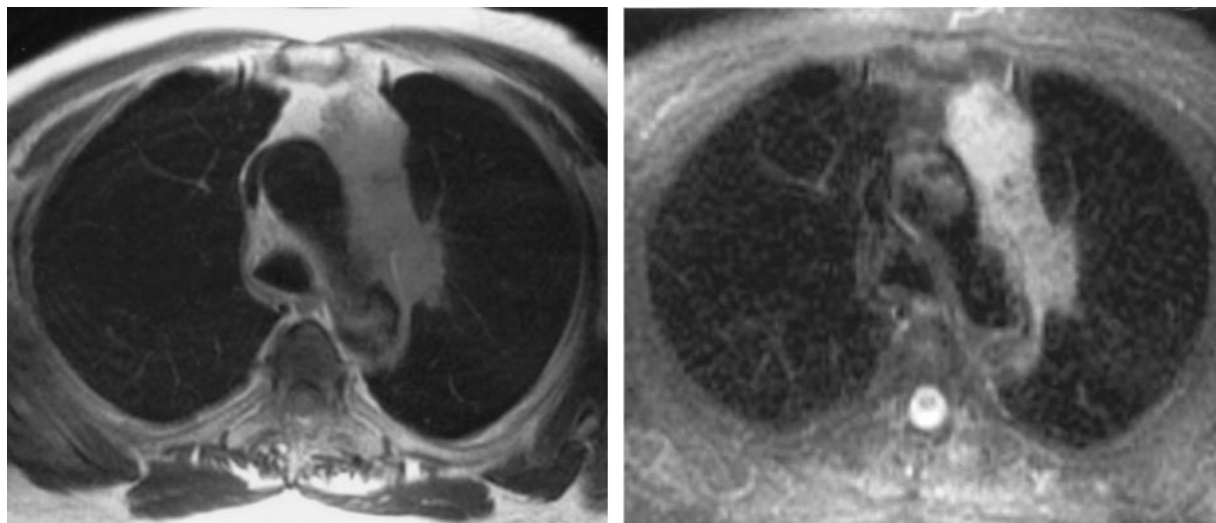


**Figure 14.** Short-axis cardiac steady-state free precession cine images (in end diastole) obtained from apex to base by using SENSE (acceleration factor = 2). Three sections were acquired per breath hold, allowing the total acquisition time to be considerably shortened.



**a.** **b.**  
**Figure 15.** Axial double (**a**) and triple (**b**) inversion-recovery images of a patient with lung cancer and mediastinal metastases. SENSE (acceleration factor = 2) was used to reduce the acquisition time from 15 seconds to 8 seconds.

relatively long acquisition times; these sequences also benefit from parallel imaging with reduced acquisition times (Fig 15) (32).

Electrocardiographic gating is a frequent source of frustration in cardiac MR imaging, particularly in patients with frequent premature ventricular contractions or other arrhythmias. Parallel imaging reduces the number of electrocardiographic triggers needed to successfully acquire an image and can thereby increase the probability of success in patients in whom gating is difficult. Parallel imaging also has something to offer for the occasional patient in whom electrocardiographic gating is completely unsuccessful: The application of high acceleration factors and relatively low spatial resolution has allowed ungated real-time cine imaging to be performed with frame rates as high as 20–30 per second (27,29,33), which is more than adequate for quantification of ejection fraction and cardiac volumes. This fast real-time imaging capability will also be important as interventional MR imaging moves into the clinical arena.

Cine phase-contrast sequences are useful for measuring blood flow in a number of circumstances, including quantification of intra- or extracardiac shunts and quantification of valvular insufficiency. Breath-hold acquisitions allow much better definition of vessel borders but are somewhat limited by temporal resolution. As noted earlier, parallel imaging should help improve the temporal resolution of these techniques and thereby improve their accuracy and reliability.

Coronary artery imaging remains a challenging aspect of cardiac MR imaging. Coronary MR angiography techniques are often divided into breath-hold and navigator-gated methods. Breath-hold methods have the advantage of speed and the opportunity for use of intravenous contrast material, but they are often limited by the spatial resolution achievable within a reasonable breath hold. Parallel imaging allows increased spatial coverage or increased spatial resolution without increasing the acquisition time, although at a cost of reduced SNR (Fig 16) (34).

### Breast Imaging

Dynamic contrast-enhanced breast MR imaging is now a common clinical technique and has demonstrated high sensitivity for detection of subtle lesions often missed at mammography. Specificity can be improved by evaluating the enhancement characteristics of these lesions over time. Three-dimensional SPGR sequences offer excellent spatial resolution, but coverage of both breasts with adequate temporal resolution has been problematic. Parallel imaging offers a solution to this problem, allowing increased spatial coverage without increasing the acquisition time so that both breasts can be evaluated with adequate temporal resolution for distinguishing benign from malignant enhancement patterns (Fig 17).

### MR Enterography and Colonography

Interest in bowel imaging with MR has increased dramatically in the past few years. The most common techniques generally employ 2D or 3D contrast-enhanced fat-saturated SPGR sequences in



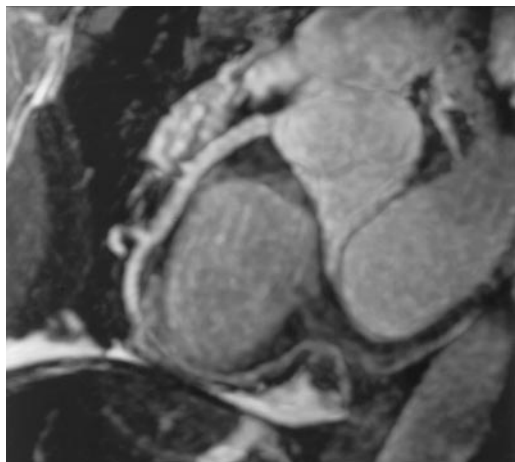


**Figure 16.** Subvolume maximum intensity projection image of the right coronary artery from nonenhanced fat-saturated steady-state free precession MR angiography performed with SENSE (acceleration factor = 2). Both spatial resolution and spatial coverage were slightly increased over those achieved with the standard acquisition.

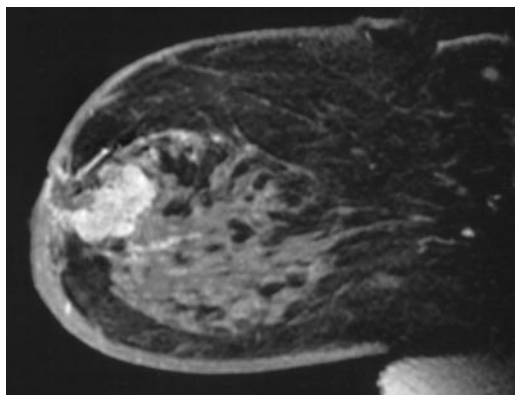


**Figure 17.** Sagittal image of a patient with residual breast carcinoma after an excisional biopsy, obtained with a dynamic contrast-enhanced 3D fat-saturated SPGR sequence. Use of SENSE (acceleration factor = 2) allowed coverage of both breasts with adequate spatial resolution and adequate temporal resolution.

conjunction with a low-signal-intensity intraluminal contrast agent, as well as bright-lumen single-shot fast SE and steady-state free precession imaging. A frequent problem with many of these studies is peristalsis, which degrades images through motion artifact. Parallel imaging can be used to reduce acquisition times and thereby diminish the amount of motion artifact (Fig 18).

### Novel Applications

Although the idea is not intuitively obvious, parallel imaging may be used to increase SNR. For example, Weiger et al (35) have shown that paral-

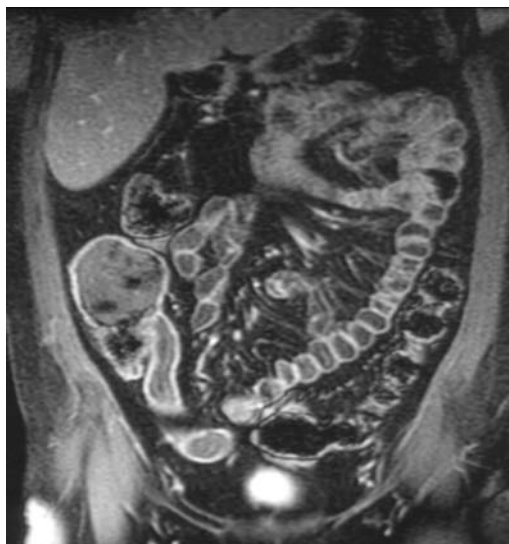


**Figure 18.** Coronal contrast-enhanced fat-saturated 2D SPGR image of a patient with Crohn disease shows mild thickening and enhancement of the terminal ileum. SENSE (acceleration factor = 2) was used to reduce the acquisition time and thereby decrease motion artifact caused by peristalsis.

lel imaging can be used to increase SNR in steady-state gradient-echo sequences by allowing the choice of a longer TR for the same acquisition time. They advocate the concept of regarding parallel imaging as an additional degree of freedom in optimizing SNR. Likewise, another strategy for increasing SNR in fast gradient-echo sequences is to use the time efficiency of parallel imaging to decrease the receiver bandwidth, thereby improving SNR.

Parallel imaging may be used to image a small FOV without wraparound artifact. Here the effective acceleration factor is 0, and the sensitivity maps are used to reconstruct an image that was acquired without reduced k-space sampling. Parallel imaging is also useful for reduction of specific absorption rate in pulse sequences with multiple echoes, high flip angles, and so on, particularly at high magnetic field strengths.

By reducing the total number of radiofrequency pulses, parallel imaging can significantly reduce the specific absorption rate; this is likely to be particularly useful in 3-T systems. Parallel imaging offers additional advantages for high-field-strength imaging (36). As the main field strength increases, T2 and T2\* generally decrease, leading to increased image blurring and artifacts in sequences with long readout echo trains (echo-planar imaging, spiral imaging, single-shot fast SE).

The use of parallel imaging techniques will minimize these effects by reducing the echo train lengths of these sequences. SNR limitations have generally prevented the use of very high  $R$  factors in parallel imaging. Wiesinger et al (37) examined the concept of ultimate SNR in terms of the coil  $g$  factor as a function of field strength and acceleration factor  $R$ . For low and moderate field strengths, the critical reduction factor (leading to exponential growth in  $g$  and diminished SNR) lies between 3 and 4. At much higher field strengths (eg, 7 T), the feasible range of acceleration factors increases markedly, suggesting that at very high field strengths parallel imaging may be even more useful.

Parallel imaging has been used in a number of ways to reduce motion artifact. For example, it is standard practice to average the signal from multiple acquisitions to reduce the effect of motion that is not consistent between acquisitions and improve SNR. Of course, use of multiple signals averaged adds considerably to the acquisition time, which is problematic in breath-hold applications. However, a parallel acquisition with two signals averaged can be performed in the same time as a single conventional acquisition and may reduce motion artifact. As noted earlier, image blurring as well as artifacts related to magnetic field inhomogeneities are prominent in long echo train sequences and can be reduced by the use of parallel imaging. A variant of parallel imaging has been applied to multishot echo-planar imaging to reduce artifacts, resulting in reduced distortion from off-resonance effects and in-plane flow (38).

Although most clinical applications of parallel imaging involve acceleration factors of 3 or less, a few investigators have demonstrated that acceptable image quality can be obtained with much higher acceleration factors (39,40). For example, Zhu et al (39) used a 32-channel coil to achieve a 16-fold acceleration while still preserving reasonable image quality.

### Limitations

Parallel imaging is a versatile technique with a large number of useful applications, as described earlier. However, it is not without limitations. The significant loss in SNR means that sequences with inherently low SNR are not good candidates for parallel imaging. Likewise, SNR limitations must be kept in mind when parallel imaging is used to improve spatial resolution. Reconstruction artifacts are occasionally problematic. Although many of these can be minimized by care-

ful attention to technique, some are unavoidable and may significantly reduce image quality. Many other techniques are available to reduce acquisition times, including partial Fourier, partial echo, use of a partial phase FOV, and decreased spatial resolution. These alternatives have their own limitations, but it is often worth exploring one or more of these options before resorting to parallel imaging.

### Conclusions

Parallel imaging constitutes a family of techniques in which the number of sampled k-space lines is reduced, often by a factor of 2 or greater, thereby significantly shortening acquisition times. These methods have a wide range of potential clinical applications, primarily involving reduction in acquisition time, improved spatial resolution, or a combination of the two. Improvements in image quality can be obtained by reducing echo train lengths of fast SE and single-shot fast SE sequences. Parallel imaging is particularly attractive for cardiac and vascular applications and will likely prove valuable as 3-T body and cardiovascular imaging moves into standard clinical practice. Limitations of parallel imaging include reduced SNR and reconstruction artifacts. It is important to consider these limitations when deciding when to employ these techniques.

### References

1. Hutchinson M, Raff U. Fast MRI data acquisition using multiple detectors. *Magn Reson Med* 1988; 6:87-91.
2. Kelton J, Magin RM, Wright SM. An algorithm for rapid acquisition using multiple receiver coils (abstr). In: *Book of abstracts: Society of Magnetic Resonance in Medicine*. Berkeley, Calif: Society of Magnetic Resonance in Medicine, 1989; 1172.
3. Kwiat D, Einav S, Navon G. A decoupled coil detector array for fast image acquisition in magnetic resonance imaging. *Med Phys* 1991;18:251-265.
4. Carlson JW, Minemura T. Imaging time reduction through multiple receiver coil data acquisition and image reconstruction. *Magn Reson Med* 1993;29: 681-687.
5. Ra JB, Rim CY. Fast imaging using subencoding data sets from multiple detectors. *Magn Reson Med* 1993;30:142-145.
6. Sodickson DK, Manning WJ. Simultaneous acquisition of spatial harmonics: fast imaging with radiofrequency coil arrays. *Magn Reson Med* 1997; 38:591-603.
7. Griswold MA, Jakob PM, Heidemann RM, et al. Generalized autocalibrating partially parallel acquisitions (GRAPPA). *Magn Reson Med* 2002;47: 1202-1210.
8. Pruessmann KP, Weiger M, Scheidegger MB, Boesiger P. SENSE: sensitivity encoding for fast MRI. *Magn Reson Med* 1999;42:952-962.

9. Pruessmann KP, Weiger M, Boesiger P. Sensitivity encoded cardiac MRI. *J Cardiovasc Magn Reson* 2001;3:1–9.
10. Weiger M, Pruessmann KP, Boesiger P. 2D SENSE for faster 3D MRI. *MAGMA* 2002;14:10–19.
11. Heidemann RM, Ozsarlak O, Parizel PM, et al. A brief review of parallel magnetic resonance imaging. *Eur Radiol* 2003;13:2323–2327.
12. Bammer R, Schoenberg SO. Current concepts and advances in clinical parallel magnetic resonance imaging. *Top Magn Reson Imaging* 2004;15(3):129–158.
13. Wilson GJ, Hoozeveen RM, Willinek WA, Muthupillai R, Maki JH. Parallel imaging in MR angiography. *Top Magn Reson Imaging* 2004;15(3):169–185.
14. Weiger M, Pruessmann KP, Kassner A, et al. Contrast-enhanced 3D MRA using SENSE. *J Magn Reson Imaging* 2000;12:671–677.
15. Maki JH, Wilson GJ, Eubank WB, Hoozeveen RM. Utilizing SENSE to achieve lower station sub-millimeter isotropic resolution and minimal venous enhancement in peripheral MR angiography. *J Magn Reson Imaging* 2002;15:484–491.
16. Muthupillai R, Vick GW, Flamm SD, Chung T. Time-resolved contrast-enhanced magnetic resonance angiography in pediatric patients using sensitivity encoding. *J Magn Reson Imaging* 2003;17:559–564.
17. Ohno Y, Kawamitsu H, Higashino T, et al. Time-resolved contrast-enhanced pulmonary MR angiography using sensitivity encoding. *J Magn Reson Imaging* 2003;17:330–336.
18. Golay X, Brown SJ, Itoh R, Melhem ER. Time-resolved contrast-enhanced carotid MR angiography using sensitivity encoding. *AJNR Am J Neuroradiol* 2001;22:1615–1619.
19. de Vries M, Nijenhuis RJ, Hoozeveen RM, de Haan MW, van Engelshoven JMA, Leiner T. Contrast-enhanced peripheral MR angiography using SENSE and multiple stations: feasibility study. *J Magn Reson Imaging* 2005;21:37–45.
20. Hu HH, Madhuranthakam AJ, Kruger DG, Huston JH 3rd, Riederer SJ. Improved venous suppression and spatial resolution with SENSE in elliptical centric 3D contrast-enhanced MR angiography. *Magn Reson Med* 2004;52:761–765.
21. Campeau NG, Huston J 3rd, Bernstein MA, Lin C, Gibbs GF. Magnetic resonance angiography at 3.0 Tesla: initial clinical experience. *Top Magn Reson Imaging* 2001;12(3):183–204.
22. Lin W, An H, Chen Y, et al. Practical considerations for 3T imaging. *Magn Reson Imaging Clin N Am* 2003;11(4):615–639.
23. Yoshioka H, Takahashi N, Yamaguchi M, Lou D, Saida Y, Itai Y. Double arterial phase dynamic MRI with sensitivity encoding for hypervascular hepatocellular carcinomas. *J Magn Reson Imaging* 2002;16:259–266.
24. van den Brink JS, Watanabe Y, Kuhl CK, et al. Implications of SENSE MR in routine clinical practice. *Eur J Radiol* 2003;46:3–27.
25. Kurihara Y, Yakushiji YK, Tani I, Nakajima Y, Van Cauteren M. Coil sensitivity encoding in MR imaging: advantages and disadvantages in clinical practice. *AJR Am J Roentgenol* 2002;178:1087–1091.
26. Zech CJ, Herrmann KA, Huber A, et al. High resolution MR imaging of the liver with T2-weighted sequences using integrated parallel imaging: comparison of prospective motion correction and respiratory triggering. *J Magn Reson Imaging* 2004;20:443–450.
27. Guttman MA, Kellman P, Dick AJ, Lederman RJ, McVeigh ER. Real-time accelerated interactive MRI with adaptive TSENSE and UNFOLD. *Magn Reson Med* 2003;50:315–321.
28. Beerbaum P, Korperich H, Gieseke J, Barth P, Peuster M, Meyer H. Rapid left-to-right shunt quantification in children by phase-contrast magnetic resonance imaging combined with sensitivity encoding. *Circulation* 2003;108:1355–1361.
29. Weiger M, Pruessmann KP, Boesiger P. Cardiac real-time imaging using SENSE. *Magn Reson Med* 2000;43:177–184.
30. Kostler H, Sandstede JJ, Lipke C, Landschutz W, Beer M, Hahn D. Auto-SENSE perfusion imaging of the whole human heart. *J Magn Reson Imaging* 2003;18(6):702–708.
31. Hunold P, Maderwald S, Ladd ME, Jellus V, Barkhausen J. Parallel acquisition techniques in cardiac cine magnetic resonance imaging using TrueFISP sequences: comparison of image quality and artifacts. *J Magn Reson Imaging* 2004;20:506–511.
32. Itskovich VV, Mani V, Mizsei G, et al. Parallel and nonparallel simultaneous multislice black-blood double inversion recovery techniques for vessel wall imaging. *J Magn Reson Imaging* 2004;19(4):459–467.
33. Wintersperger BJ, Nikolaou K, Dietrich O, et al. Single breath-hold real-time cine MR imaging: improved temporal resolution using generalized autocalibrating partially parallel acquisition algorithm. *Eur Radiol* 2003;13(8):1931–1936.
34. Dirksen MS, Lamb HJ, Doornbos J, Bax JJ, Jukema JW, de Roos A. Coronary magnetic resonance angiography: technical developments and clinical applications. *J Cardiovasc Magn Reson* 2003;5(2):365–386.
35. Weiger M, Boesiger P, Hilfiker PR, Weishaupt D, Pruessmann KP. Sensitivity encoding as a means of enhancing the SNR efficiency in steady-state MRI. *Magn Reson Med* 2005;53:177–185.
36. Pruessmann KP. Parallel imaging at high field strength: synergies and joint potential. *Top Magn Reson Imaging* 2004;15(4):237–244.
37. Wiesinger F, Boesiger P, Pruessmann KP. Electrodynamics and ultimate SNR in parallel MR imaging. *Magn Reson Med* 2004;52:376–390.
38. Kellman P, McVeigh ER. Ghost artifact cancellation using phased array processing. *Magn Reson Med* 2001;46:335–343.
39. Zhu Y, Hardy CJ, Sodickson DK, et al. Highly parallel volumetric imaging with a 32-element RF coil array. *Magn Reson Med* 2004;52:869–877.
40. Hardy CJ, Darrow RD, Saranathan M, et al. Large field of view real time MRI with a 32 channel system. *Magn Reson Med* 2004;52:878–884.